ChemComm

RSC Publishing

COMMUNICATION

View Article Online
View Journal | View Issue

Adsorption and dehydrogenation of tetrahydroxybenzene on Cu(111)†

Cite this: *Chem. Commun.*, 2013, **49**, 9308

Received 5th July 2013,
Accepted 9th August 2013

DOI: 10.1039/c3cc45052j

www.rsc.org/chemcomm

Fabian Bebensee,[a] Katrine Svane,[a] Christian Bombis,[a] Federico Masini,[a] Svetlana Klyatskaya,[b] Flemming Besenbacher,[a] Mario Ruben,[bc] Bjørk Hammer[a] and Trolle Linderoth*[a]

Adsorption of tetrahydroxybenzene (THB) on Cu(111) and Au(111) surfaces is studied using a combination of STM, XPS, and DFT. THB is deposited intact, but on Cu(111) it undergoes gradual dehydrogenation of the hydroxyl groups as a function of substrate temperature, yielding a pure dihydroxy-benzoquinone phase at 370 K. Subtle changes to the adsorption structure upon dehydrogenation are explained from differences in molecule–surface bonding.

The fabrication of supramolecular structures on surfaces[1] through non-covalent interactions[2] has recently received tremendous interest. To rationalise and exploit this approach, it is essential that the chemical state of the molecular building blocks on the surface is known, which can be complicated by degradation/reaction during deposition or after adsorption on the surface.[3] Dehydrogenation reactions are particularly interesting in this respect since they can *e.g.* remove or create the possibility to establish hydrogen bonds or change the bonding of molecules to the substrate.[4] Dehydrogenation is well known to occur for carboxylic acids[5] including amino acids,[6] but has also been observed for less acidic hydroxyl groups, *e.g.* for alcohols[7] or even terminal acetylenes.[8]

In general, there is a need to expand the knowledge base for molecular dehydrogenation reactions on surfaces and improve our understanding of the conditions under which dehydrogenation occurs. Dehydrogenation and similar chemical changes are often linked to pronounced structural changes in the supramolecular assemblies which can be observed using Scanning Tunneling Microscopy (STM).[1a,4c,9] Here we investigate a case of dehydrogenation for a comparatively simple molecule 1,2,4,5-tetrahydroxybenzene[10] (THB) where pronounced dehydrogenation is only accompanied by subtle changes to the adsorption structures. Adsorption of THB and related molecules was studied previously in relation to metal coordination[11] or covalent networks[12] on surfaces. From X-ray Photoelectron Spectroscopy (XPS) we show that THB is deposited intact on Au(111), but on Cu(111) it gradually undergoes thermally activated dehydrogenation of its hydroxyl groups, eventually yielding dihydroxy-benzoquinone at 370 K. The energetics of the dehydrogenation process is elucidated from Density Functional Theory (DFT) calculations emphasizing the importance of the entropic contribution of desorbed hydrogen. The subtle changes to the adsorption structure observed in STM images upon dehydrogenation are explained from differences in molecule–surface bonding.

The experiments were conducted in a UHV-setup equipped with an Aarhus STM and *in situ* facilities for XPS (see ESI† for details). Fig. 1a depicts the adsorption structure observed after deposition of

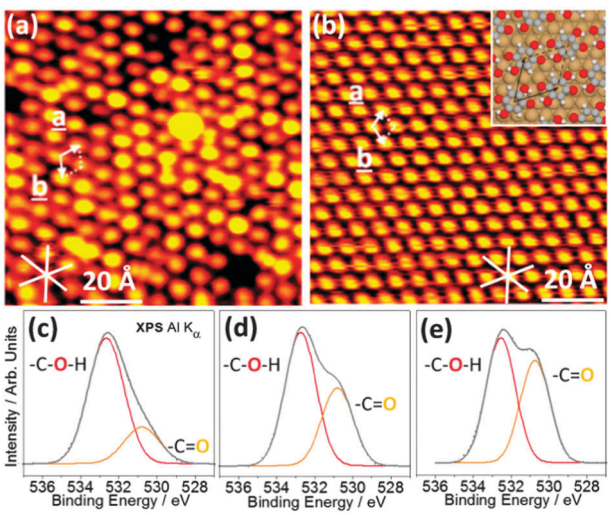

Fig. 1 (a and b) STM images obtained after deposition of THB on Cu(111). (a) As-deposited at 300 K and (b) after annealing to 370 K (I_T 0.35 nA, U_T −1.25/−1.4 V). The inset in (b) shows a model for the annealed structure (*cf.* Fig. S5, ESI†). (c–e) XP spectra of the O 1s region after THB deposition. (c) After deposition at 115 K (acquired at this temperature), (d) after deposition at RT and (e) after annealing to 370 K (d and e acquired at 320 K).

[a] *Sino-Danish Center for Molecular Nanostructures on Surfaces, Interdisciplinary Nanoscience Center (iNANO) and Department of Physics and Astronomy, Aarhus University, Aarhus C, Denmark. E-mail: trolle@inano.au.dk*
[b] *Karlsruhe Institute of Technology (KIT), Institut für Nanotechnologie, Karslruhe, Germany*
[c] *IPCMS-CNRS, Université de Strasbourg, Strasbourg, France*

† Electronic supplementary information (ESI) available: Experimental and computational details, STM and XPS data for DHBQ on Cu(111) and the synchrotron based XP spectrum of THB/Cu(111) at RT. See DOI: 10.1039/c3cc45052j

THB on Cu(111) at room temperature (RT, 300 K). The structure consists of protrusions in a hexagonal arrangement described by a unit cell with side lengths of 7.5 Å oriented at angles of $\pm(12 \pm 2^{\circ})$ with respect to the high symmetry $\langle 10{-}1 \rangle$ directions of the Cu substrate. Interestingly, the protrusions show different STM contrast with a variation in the apparent height of 0.28 ± 0.07 Å (a few point defects are visible which lie outside this range). Annealing to 370 K results in the adsorption structure shown in Fig. 1b, which has the same hexagonal unit cell size (7.5 Å) but a slightly different orientation with respect to the substrate of $\pm(19 \pm 2^{\circ})$ (in rare cases $0 \pm 2^{\circ}$). Most notably, the structure is now smooth with all protrusions showing the same apparent height. Two questions arise from these STM images: what is the origin of the inhomogeneity in the as-deposited structure (Fig. 1a) and what is the molecular level effect of the annealing which removes this inhomogeneity? To probe the chemical state of the molecules in the respective situations, we employed XPS. Fig. 1c–e presents spectra of the O 1s region recorded after deposition of THB on a Cu(111) substrate held at 115 K (c) as well as at RT (d) and after annealing to 370 K (e). All three spectra can be fitted with two contributions at binding energies (BEs) of 532.6 ± 0.1 eV and 530.8 ± 0.1 eV, respectively. As the four oxygen atoms of THB are chemically equivalent, the observation of two features in the O 1s region suggests partial dehydrogenation. Hence, the high BE feature is ascribed to oxygen in hydroxyl groups and the low BE feature to oxygen in carbonyl groups in agreement with the literature.[9c] The sequence of spectra shows an increasing contribution from the low BE component which increases from 22% (c) over 37% (d) to 45% (e). The level of dehydrogenation thus increases with increasing substrate temperature, suggesting a thermally activated process.

As control experiments, we deposited both THB and DHBQ (2,5-dihydroxy-benzoquinone; a related compound in which two hydroxyls are replaced by carbonyl groups in the *para* position) on an inert Au(111) substrate (see ESI† concerning the possibility of an *o*-benzoquinone product). The STM images in Fig. 2a and d reveal virtually identical structures for THB and DHBQ adsorbed on Au(111) at RT: both form hexagonal structures with a unit cell size of 7.5 Å oriented at $\pm(20 \pm 2^{\circ})$ with respect to the substrate's high symmetry directions. The XP spectrum of the O 1s region of THB (Fig. 2b) exhibits a single peak at a BE of 532.4 eV, while DHBQ (Fig. 2e) features two peaks of almost equal intensity at BEs of 532.7 eV and 531.1 eV, respectively. The two spectra correlate well with the molecular structures, establishing the assignment of the high/low BE features to the hydroxyl/carbonyl groups on Au(111) and corroborating the assignment done above on Cu(111). The corresponding C 1s spectra shown in Fig. 2c and f are almost identical and exhibit two features at BEs of 285.2 eV and 283.8 eV (THB)/283.9 eV (DHBQ) with an intensity ratio of $\sim 2:1$ in favour of the high BE feature. The high intensity feature is assigned to the 4 carbons attached to oxygens in hydroxyl or carbonyl groups, which are expected to have similar BE's, and the low intensity feature to the 2 carbons not connected to oxygen (see ESI† for comparison to calculated core level shifts). The control experiments thus establish that THB is sublimated intact onto the surface (also X-ray beam damage does not occur). The spectrum of DHBQ on Au(111) (Fig. 2e) bears very close resemblance to that of annealed THB on Cu(111) (Fig. 1e). Further control experiments with DHBQ adsorbed on Cu(111) are also in good agreement with annealed THB regarding STM monolayer structure and XPS spectra (see ESI†). We therefore conclude that annealing THB on Cu(111) to 370 K results in formation of DHBQ *via* dehydrogenation. Based on literature reports, the abstracted hydrogen is thought to desorb recombinatively from the surface.[13]

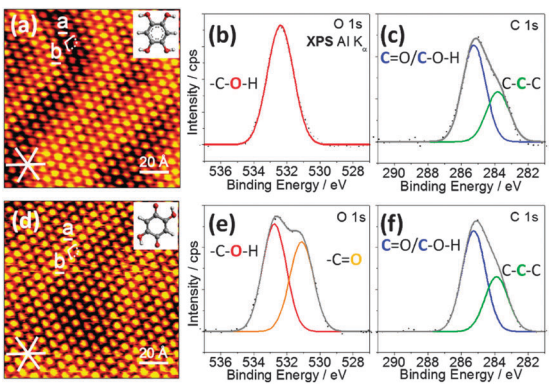

Fig. 2 Left: STM images of THB (a) and DHBQ (d) adsorbed on Au(111) at RT (I_T 0.35/0.37 nA, U_T −1.36/−1.4 V). Insets show molecular models of the respective compounds. The observed height modulation is caused by the Au(111) herringbone reconstruction. Right: corresponding XP spectra of the O 1s and C 1s regions for THB (b and c) and DHBQ (e and f).

To clarify the driving forces for the observed dehydrogenation and to establish the origin of the different contrasts for as-deposited THB, we performed DFT calculations. The DFT calculations included dispersive effects by using the *meta*-GGA functional M06-L (*cf.* ESI† for details).[14] The resulting optimised adsorption geometries for THB and DHBQ on Cu(111) are shown in Fig. 3a and b and the corresponding energy landscape in Fig. 3d. The energy calculations demonstrate that the dehydrogenation results in a net increase in enthalpy (black bars in Fig. 3d). In many cases, a strong enthalpic driving force for dehydrogenation renders it unnecessary to consider entropy effects.[15] Here, however, the entropy of the desorbed hydrogen molecules abstracted from THB plays an important role in the thermodynamics. A hydrogen molecule desorbed from the surface after dehydrogenation has high entropy, in particular at the low pressure in the UHV chamber. A conservative estimate for the pressure during our experiments is 10^{-9} mbar, corresponding to an entropy contribution of −1.11 eV per H_2 to the free energy at RT. Another contribution that is often neglected is the change in vibrational zero point energy resulting from a reaction. Here, we estimate this correction to be −0.17 eV (*cf.* ESI†). Adding these two contributions to establish the free energy landscape (red bars) shows that the system moves down in free energy by dehydrogenation.

In its optimised adsorption geometry, THB adsorbs with the plane of the carbon ring parallel to the surface, at a distance of 2.9 Å above the surface, and with the centre of the ring located above a bridge site. DHBQ also adsorbs at the bridge site, but the distance between the carbon ring and the surface is shortened to 2.3 Å. The calculations show that the carbonyl bonds in DHBQ are elongated from 1.23 Å (typical of a double bond) when the molecule is in the gas phase, to 1.31 Å (an intermediate between single and double bonds), when it is adsorbed on the surface. This bond lengthening indicates that the bond between the carbonyl oxygen of DHBQ and the surface plays the role of the O–H bond found in THB. In this way

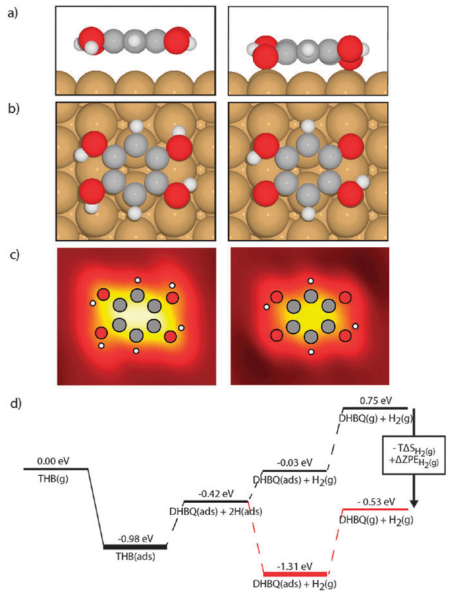

Fig. 3 Calculated adsorption geometry for THB (left) and DHBQ (right) on Cu(111) in side (a) and top (b) view, simulated STM images (c) and the energy landscape (d) relative to THB in the gas phase. Black bars represent enthalpies and red bars represent free energies at RT.

the conjugated π-system of the carbon ring in THB can remain relatively intact when the molecule is dehydrogenated on the surface. A strong interaction between the carbonyl oxygen and the Cu surface is supported by the XPS measurements showing that the O 1s BE in the carbonyl group is measurably higher on Au(111) (531.1 eV) compared to that on Cu(111) (530.8 eV), while the hydroxyl O 1s BE is the same. Overall, the stronger interaction between the carbonyl oxygen and the surface, compared to the hydroxyl–surface interaction, brings the dehydrogenated DHBQ molecule closer to the surface compared to THB. Simulated STM images based on the Tersoff–Hamann model (Fig. 3c) show a lower apparent height for DHBQ than for THB reflecting mainly these different adsorption heights.

The change in the STM images observed upon annealing can now be rationalised: at RT, a mixture of THB and DHBQ exists, as implied by the appearance of features with different apparent height in the STM images. Quantitative analysis of STM images in Fig. 1a shows that the protrusions exhibit a variation in apparent heights rather than two distinct levels, possibly due to locally varying bonding configurations. We estimate the fraction of DHBQ (dim protrusions) to lie in the range 0.5–0.75. This range corresponds to dehydrogenation of 31 ± 7% of the hydroxyl groups consistent with XPS (Fig. 1b and ESI† Section 3). The DHBQ and THB species are thoroughly intermixed indicating a homogenous level of dehydrogenation across the surface. Annealing the sample to 370 K leads to further dehydrogenation, converting all THB molecules into DHBQ. A suggested structural model for the DHBQ overlayer is shown in Fig. 1c and Fig. S5 (ESI†). The model is based on the optimal hydrogen bonding pattern found from DFT calculations in the gas phase using the experimentally observed unit cell. This structure was subsequently transferred to a Cu substrate and relaxed, allowing formation of Cu–carbonyl bonds. The optimised structure is comprised of parallel rows of molecules which are inter-linked within the rows *via* double hydrogen bonds. The origins of the slight change in rotational orientation between the mixed DHBQ–THB and pure DHBQ overlayers cannot be quantitatively assessed due to the many inequivalent bonding situations in the large computational unit cell, but we speculate that the rotation occurs to optimise the molecule–substrate interaction arising from an increased number of Cu–carbonyl bonds.

We acknowledge support from the Danish National Research Foundation, the Danish Council for Independent Research, the Marie-Curie networks SMALL and MONET, the Lundbeck Foundation, DCSC, and the Alexander von Humboldt-Foundation.

Notes and references

1 (*a*) J. A. A. W. Elemans, S. B. Lei and S. De Feyter, *Angew. Chem., Int. Ed.*, 2009, **48**, 7298–7332; (*b*) G. Franc and A. Gourdon, *Phys. Chem. Chem. Phys.*, 2011, **13**, 14283–14292.
2 J. V. Barth, *Annu. Rev. Phys. Chem.*, 2007, **58**, 375–407.
3 (*a*) F. Bebensee, C. Bombis, S.-R. Vadapoo, J. R. Cramer, F. Besenbacher, K. V. Gothelf and T. R. Linderoth, *J. Am. Chem. Soc.*, 2013, **135**, 2136–2139; (*b*) M. Kittelmann, P. Rahe, A. Gourdon and A. Kuhnle, *ACS Nano*, 2012, **6**, 7406–7411.
4 (*a*) L. Bartels, *Nat. Chem.*, 2010, **2**, 87–95; (*b*) A. M. Beatty, *Coord. Chem. Rev.*, 2003, **246**, 131–143; (*c*) A. C. Papageorgiou, S. Fischer, J. Reichert, K. Diller, F. Blobner, F. Klappenberger, F. Allegretti, A. P. Seitsonen and J. V. Barth, *ACS Nano*, 2012, **6**, 2477–2486.
5 (*a*) M. E. Canas-Ventura, F. Klappenberger, S. Clair, S. Pons, K. Kern, H. Brune, T. Strunskus, C. Woll, R. Fasel and J. V. Barth, *J. Chem. Phys.*, 2006, 125; (*b*) M. N. Faraggi, C. Rogero, A. Arnau, M. Trelka, D. Ecija, C. Isvoranu, J. Schnadt, C. Marti-Gastaldo, E. Coronado, J. M. Gallego, R. Otero and R. Miranda, *J. Phys. Chem. C*, 2011, **115**, 21177–21182; (*c*) L. Kanninen, N. Jokinen, H. Ali-Loytty, P. Jussila, K. Lahtonen, M. Hirsimaki, M. Valden, M. Kuzmin, R. Parna and E. Nommiste, *Surf. Sci.*, 2011, **605**, 1968–1978; (*d*) N. Lin, A. Dmitriev, J. Weckesser, J. V. Barth and K. Kern, *Angew. Chem., Int. Ed.*, 2002, **41**, 4779–4783; (*e*) M. Matena, M. Stohr, T. Riehm, J. Bjork, S. Martens, M. S. Dyer, M. Persson, J. Lobo-Checa, K. Muller, M. Enache, H. Wadepohl, J. Zegenhagen, T. A. Jung and L. H. Gade, *Chem.–Eur. J.*, 2010, **16**, 2079–2091.
6 (*a*) T. Eralp, A. Shavorskiy, Z. V. Zheleva, G. Held, N. Kalashnyk, Y. X. Ning and T. R. Linderoth, *Langmuir*, 2010, **26**, 18841–18851; (*b*) V. Humblot, C. Methivier, R. Raval and C. M. Pradier, *Surf. Sci.*, 2007, **601**, 4189–4194.
7 (*a*) R. Pawlak, S. Clair, V. Oison, M. Abel, O. Ourdjini, N. A. A. Zwaneveld, D. Gigmes, D. Bertin, L. Nony and L. Porte, *ChemPhysChem*, 2009, **10**, 1032–1035; (*b*) S. Polmann, A. Bayer, C. Ammon and H. P. Steinruck, *Z. Phys. Chem.*, 2004, **218**, 957–971; (*c*) C. Ammon, A. Bayer, G. Held, B. Richter, T. Schmidt and H. P. Steinruck, *Surf. Sci.*, 2002, **507**, 845–850.
8 Y. Q. Zhang, N. Kepcija, M. Kleinschrodt, K. Diller, S. Fischer, A. C. Papageorgiou, F. Allegretti, J. Bjork, S. Klyatskaya, F. Klappenberger, M. Ruben and J. V. Barth, *Nat. Commun.*, 2012, **3**, 1286.
9 (*a*) N. Lin, D. Payer, A. Dmitriev, T. Strunskus, C. Woll, J. V. Barth and K. Kern, *Angew. Chem., Int. Ed.*, 2005, **44**, 1488–1491; (*b*) M. Ruben, D. Payer, A. Landa, A. Comisso, C. Gattinoni, N. Lin, J. P. Collin, J. P. Sauvage, A. De Vita and K. Kern, *J. Am. Chem. Soc.*, 2006, **128**, 15644–15651; (*c*) S. Stepanow, T. Strunskus, M. Lingenfelder, A. Dmitriev, H. Spillmann, N. Lin, J. V. Barth, C. Woll and K. Kern, *J. Phys. Chem. B*, 2004, **108**, 19392–19397.
10 C. A. Hansen and J. W. Frost, *J. Am. Chem. Soc.*, 2002, **124**, 5926–5927.
11 H. M. Zhang, W. Zhao, Z. X. Xie, L. S. Long, B. W. Mao, X. Xu and L. S. Zheng, *J. Phys. Chem. C*, 2007, **111**, 7570–7573.
12 (*a*) L. M. Lanni, R. W. Tilford, M. Bharathy and J. J. Lavigne, *J. Am. Chem. Soc.*, 2011, **133**, 13975–13983; (*b*) N. A. A. Zwaneveld, R. Pawlak, M. Abel, D. Catalin, D. Gigmes, D. Bertin and L. Porte, *J. Am. Chem. Soc.*, 2008, **130**, 6678–6679.
13 T. Kammler and J. Kuppers, *J. Chem. Phys.*, 1999, **111**, 8115–8123.
14 L. Ferrighi, G. K. H. Madsen and B. Hammer, *J. Chem. Phys.*, 2011, 135.
15 (*a*) S. Clair, S. Pons, S. Fabris, S. Baroni, H. Brune, K. Kern and J. V. Barth, *J. Phys. Chem. B*, 2006, **110**, 5627–5632; (*b*) T. Classen, M. Lingenfelder, Y. Wang, R. Chopra, C. Virojanadara, U. Starke, G. Costantini, G. Fratesi, S. Fabris, S. de Gironcoli, S. Baroni, S. Haq, R. Raval and K. Kern, *J. Phys. Chem. A*, 2007, **111**, 12589–12603.

